

Magnetic ordering in the randomly mixed quadratic-layer antiferromagnet with competing anisotropies $K_2Co_xFe_{1-x}F_4$

W. A. H. M. Vlak and E. Frikkee

Netherlands Energy Research Foundation ECN, P.O. Box 1, NL-1755 ZG Petten, The Netherlands

A. F. M. Arts and H. W. de Wijn

Fysisch Laboratorium, Rijksuniversiteit Utrecht, P.O. Box 80 000, NL-3508 TA Utrecht, The Netherlands

(Received 15 May 1985; revised manuscript received 27 November 1985)

The magnetic ordering in the randomly mixed quadratic-layer antiferromagnet with competing anisotropies $K_2Co_xFe_{1-x}F_4$ is studied with neutron scattering. For $x=0.18$, just below the multicritical concentration $x_c=0.22$, the critical fluctuations are suppressed and the sublattice magnetization increases only slowly with decreasing temperature, indicative of a crossover from two-dimensional (2D) Ising to 2D XY behavior near x_c . For $x=0.27$, two successive transitions are observed, at $T_N=64.4\pm 0.5$ K and $T_L=27\pm 2$ K. Between T_N and T_L the spin components along the tetragonal axis order. At T_L the oblique antiferromagnetic phase is entered, without appreciably affecting the axial order. The transition at T_L exhibits unusually slow critical fluctuations. The systems with $x=0.12$ and 0.55 , at considerable distance from x_c , acquire the K_2FeF_4 and K_2CoF_4 magnetic structures, respectively.

I. INTRODUCTION

Random antiferromagnets with competing spin anisotropies have composition-temperature phase diagrams in which a phase with coexisting order parameters separates the phases characterized by order along a preferential axis of a constituent magnetic ion. This new so-called oblique antiferromagnetic (OAF) phase has been investigated with both molecular-field¹ and renormalization-group² methods, and in real cases its existence has been verified in a limited number of three-dimensional³⁻⁵ (3D) and two-dimensional⁶⁻⁹ (2D) systems. In this paper, we report on a neutron-diffraction investigation of the randomly mixed quadratic-layer antiferromagnet $K_2Co_xFe_{1-x}F_4$ at various compositions. Principal points of interest will be the ordering upon entering the OAF phase and the ordering in the vicinity of the multicritical point, for which crossover in critical behavior is hard to detect in 3D systems.

The end members K_2CoF_4 and K_2FeF_4 both are well-studied quadratic-layer antiferromagnets. K_2CoF_4 , the archetypal 2D Ising antiferromagnet, achieves long-range order (LRO) with the Co spins pointing along the tetragonal axis (axial or A phase) at $T_N=107.85\pm 0.05$ K.¹⁰ K_2FeF_4 has Heisenberg exchange with additional single-ion anisotropies so as to leave the Fe spins along one of the in-layer magnetic axes below $T_N=63.0\pm 0.3$ K.¹¹ The stacking of the layers is unique, and the K_2FeF_4 structure thus comes in two domain types. This ordered phase is frequently referred to as the planar or PL phase, although at low temperatures the quartic in-layer anisotropy invokes a spin-wave energy gap of no less than 2.3 ± 0.1 meV and the transition is close to ideal Ising character. The phase diagram of $K_2Co_xFe_{1-x}F_4$ has already been

examined with neutron diffraction.^{7,8} The multicritical point is located at $x_c=0.22$ and $T_c=57$ K.⁷ The system has further been investigated with Raman scattering,⁹ addressing the excitations, and Mössbauer spectroscopy.^{12,13} Both compositions with $x < x_c$ and $x > x_c$ will be of concern below. On the Fe-rich side near x_c , $K_2Co_xFe_{1-x}F_4$ appears to exhibit crossover from 2D Ising to 2D XY, leading to suppression of the critical fluctuations and slow development of the sublattice magnetization. On the Co-rich side, a well-defined transition between the A and OAF phases is observed,^{7,8} but off-diagonal coupling between the axial and transverse spin components slows down the transverse critical fluctuations when the axial components have already become ordered. Such a coupling is also inferred to be present, despite the high crystal symmetry, from the discontinuities of the slopes of the phase lines at the multicritical point.

II. PRELIMINARIES AND EXPERIMENTAL DETAILS

Four single crystals of $K_2Co_xFe_{1-x}F_4$, typically $3\times 5\times 10$ mm³ in volume and with a mosaic spread of about 10 minutes of arc, were grown with the Czochralski pulling technique. With atomic-absorption spectroscopy the average concentrations x were determined to be 0.55 ± 0.02 , 0.27 ± 0.02 , 0.18 ± 0.03 , and 0.12 ± 0.03 . The composition gradient is less than 0.01 in x over the length of the sample. The homogeneity was, for a representative sample, investigated with a scanning electron microscope with a resolution of 40 μ m, and also found to be better than 0.01 in x . The neutron-diffraction experiments were performed on a double-axis diffractometer at the High-Flux Reactor in Petten. The incident beam, having a wavelength of 1.479 Å, was selected with a Zn (002)

TABLE I. Experimental and calculated intensities of Bragg reflections ($10l$) for $K_2Co_xFe_{1-x}F_4$. Experimental errors are typically a few percent. The calculated results apply to equally populated domains.

		(100)	(101)	(102)	(103)
Experimental					
$x=0^a$	$T=4.2$ K	1.0	0.15	1.0	0.32
$x=0.12$	$T=4.2$ K	1.00	0.15	0.73	0.25
$x=0.18$	$T=4.2$ K	1.00	0.09	0.68	0.11
$x=0.27$	$T=4.2$ K	1.00	0.60	0.57	0.26
	$T=30-60$ K	1.00	0.70	0.46	0.17
	Increase below T_L^b	1.0	0.3	0.8	0.5
$x=0.55$	$T=4.2$ K	1.00	0.78	0.53	0.28
Calculated					
$S_{Co,Fe} c$ axis		1.00	0.74	0.37	0.17
$S_{Co,Fe} a$ or b axis	F^c	1.00	0.15	0.67	0.31
	AF^d	0.00	0.89	0.30	0.46

^aReference 11.

^bCompared to 45 K.

^cSpins form ferromagnetic sheets through the preferred direction and the c axis, as in K_2FeF_4 .

^dSame, but antiferromagnetic sheets.

monochromator. The collimation employed was 30' horizontal in front of the monochromator, 30' vertical between monochromator and sample, and 30' horizontal and vertical in front of the detector. The samples were mounted in such a way as to allow diffraction in the (a^* , c^*) plane in reciprocal space. The experimental resolution [full width at half maximum (FWHM)] near (100) was 0.044 \AA^{-1} along the a^* axis and 0.008 \AA^{-1} along the c^* axis. At 4.2 K the lattice parameters range, with increasing x from $a=5.84$ to 5.79 \AA , and from $c=12.88$ to 12.94 \AA .

The low-temperature magnetic structure was derived from the intensities of the magnetic reflections ($10l$), with the indexing referring to the magnetic unit cell. These reflections alternately originate from the two domain types. It is recalled that the intensity of the (100) reflection is, irrespective of x , a direct measure of the *magnitude* of the sublattice magnetization projected onto the (b,c) plane, while the (101) intensity primarily reflects the *direction* in the (a,c) plane. Bragg intensities normalized to (100) calculated on the assumption of equally populated domains for relevant 3D magnetic structures are tabulated in Table I. It is noted that the magnetic form factors of Fe^{2+} and Co^{2+} do not differ to the extent of significantly affecting the calculated ratios.

Two-dimensional magnetic correlations were studied by tracking the intensity distribution along and across the ridge $Q=(1,0,\xi)$, with ξ variable. At the position $\xi=0.4$ along the ridge the wave vector k_f of the scattered neutrons is directed along the ridge, thus making the quasi-static and quasielastic approximations close to being ideally satisfied.¹⁴ The ridge intensity is quite generally brought about by three distinct phenomena dependent on x and the temperature, all of which are of relevance below: critical scattering near T_N , which at $\xi=0.4$ approximately scales with the combination $\chi_{bb} + \chi_{cc}$ of the

generalized susceptibilities, 2D Bragg scattering owing to LRO achieved by individual layers, and 2D spin-wave scattering.

III. EXPERIMENTAL RESULTS

A. Order in 3D

In Fig. 1 we present the temperature dependence of the intensities of the ($10l$) magnetic reflections, with $l=0, 1, 2$, and 3, for $x=0.12, 0.18, 0.27$, and 0.55. With the exception of $x=0.18$, the Bragg peaks are resolution-limited both in the a^* and c^* directions, while the transitions to 3D LRO occur at well-defined temperatures, with a minor smearing ($\Delta T_N \approx 0.5$ K) presumably caused by the concentration gradients. The measured relative intensities for all four compositions are, for representative temperatures, collected in Table I. For $x=0.12$, a repopulation over the domain types of order 10% is observed when cooling from T_N to 4.2 K, a phenomenon observed earlier in K_2FeF_4 .¹¹ The relative intensities for $x=0.55$ are at all temperatures below T_N consistent with perfect alignment of the spins along the tetragonal axis. For Co spins at the relevant concentration, this indeed is the orientation expected. Mössbauer spectroscopy¹² performed on the same specimen has undisputably shown that the Fe spins also point along the c axis. The $x=0.55$ system is thus in the A phase below T_N . Combining diffraction and NMR data,¹⁵ we similarly conclude that the $x=0.12$ system orders in the PL phase, i.e., both the Co and Fe spins are directed along an in-layer magnetic axis. The transitions in the $x=0.55$ and 0.12 systems are of regular 2D Ising character, as appears from fitting a power law of the form $[B(1-T/\bar{T}_N)^\beta]^2$ to the integrated (100) Bragg intensity. In the fit, the critical exponent β , the mean tran-

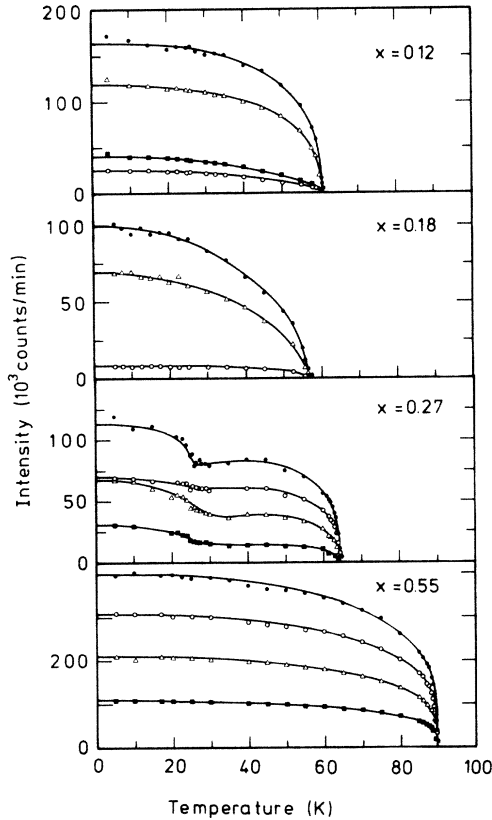


FIG. 1. Temperature dependence of the intensities of magnetic Bragg reflections $(10l)$ for various x . ●, ○, △, and ■ refer to $l=0, 1, 2,$ and $3,$ respectively. For $x=0.18,$ the (101) and (103) intensities coincide within errors, and for clarity the data points of the latter are omitted.

sition temperature $\bar{T}_N,$ the width $\sigma(\text{FWHM})$ of a Gaussian distribution of $T_N,$ and B are taken as adjustable parameters. The results are $\beta=0.13\pm 0.02$ and $\bar{T}_N=89.6\pm 0.5$ K for $x=0.55,$ and $\beta=0.16\pm 0.02$ and $\bar{T}_N=60.6\pm 0.5$ K for $x=0.12,$ while σ ranges between 1 and 2 K. The power law was found to hold down to $0.85\bar{T}_N.$ We note that adopting $\sigma=0$ would have increased the output values of β by about 0.02.

The behavior of the samples with x near x_c is in different nature. The 3D order parameter in the $x=0.18$ system develops only gradually with decreasing temperature, and the transition, occurring at 57 ± 2 K, is only marginally defined. The $(10l)$ scattering intensities at 4.2 K (Table I), particularly the (102) intensity in relation to $(100),$ however, indicate that the system has entered the PL phase. For a precise determination of the magnetic structure we again resort to NMR,¹⁵ which shows that both Co and Fe spins are aligned according to the K_2FeF_4 structure all the way down to 4.2 K within a few degrees of arc. The Bragg intensities for $x=0.18$ cannot be interpreted in terms of the usual critical behavior. If a power law of the above form were adopted, it would yield $\beta=0.18$ with an unrealistic spread σ in T_N of about 10 K, or in case σ is set to 0, the physically unrealistic value

$\beta=0.46.$ An apparent increase in β upon approaching x_c has also been observed in another 2D system with competing anisotropies, viz., $\text{K}_2\text{Mn}_{1-x}\text{Fe}_x\text{F}_4.$ ⁶ The difficulty of the system to acquire order clearly is related to the proximity of the OAF phase. A further indication for this is found in a slight increase of the scattering intensity of the (100) reflection in the wings along the c^* direction upon cooling to 15 K, reflecting a loss of interlayer correlation. It seems plausible that the system, while remaining in the PL phase, is closer to the boundary between the PL and OAF phases the lower the temperature.

In contrast to the other three specimens, the one with composition $x=0.27,$ ⁷ which is ordered below $T_N=64.4\pm 0.5$ K, exhibits a distinct second rise of the $(10l)$ Bragg intensities below $T_L=27\pm 2$ K (Fig. 1). In view of the steepness of the phase boundary (T_L decreases by 8 K per percent increase of x) and the presence of concentration variations (of order 0.01 in x), the observed rise at T_L is consistent with a sharp transition, a conclusion corroborated by Mössbauer spectroscopy.¹² Apparently, the magnetic ordering takes place in two successive stages. The transition at T_N is of 2D Ising nature, as is borne out by $\beta=0.15\pm 0.02.$ The first stage of the ordering is virtually completed at 45 K, and in the regime $T_L < T < T_N$ the system is in the A phase (cf. Table I). In the second stage of the ordering, below $T_L,$ the in-layer components of the spins also acquire 3D LRO, as appears from the increments of the intensities of the four reflections observed (cf. Table I), i.e., the system is in the OAF phase. Note that the contributions of the parallel and transverse components to the scattering are simply additive, provided the four domain types of the OAF phase are equally populated. The (100) intensity is already of substantial size at 45 K when compared to 5 K, inferring the axial components of the Fe spins to order simultaneously with the Co spins. Upon assuming 3D collinear ordering of Fe and Co spins, a more detailed analysis then indicates the axial components to remain constant below 45 K, and the transverse components to grow below 27 K. The tilt angle ϕ relative to the c axis is found to amount to $28^\circ\pm 5^\circ$ at 5 K. This result is, however, an average over true orientations of the Co and Fe spins. Mössbauer spectroscopy has established the Fe spins to deflect by as much as 52° at 5 K.¹² The slight decrement of the intensities when approaching T_L from above presumably reflects that transverse fluctuations affect the 3D axial order to some extent.

The above experiments were performed following slow cooling of the sample (< 1 K/min) from above T_N to ensure optimum 3D ordering. Subsequent rapid temperature changes below T_N did not alter the interlayer order. Relaxation was in fact, not observed to occur on a time scale of 10 h. Fast cooling (> 3 K/min) through $T_N,$ on the other hand, prevents the attainment of 3D order in the $x=0.55$ sample to some degree, an effect reminiscent of what has been observed in $\text{K}_2\text{CoF}_4.$ ¹⁶ Below $T_N,$ we further observed superlattice scattering at $(10l)$ with l a half-integer of intensity less than 1 part in 10^3 relative to $(100),$ i.e., in minor parts of the sample the stacking of next-nearest-neighbor layers is antiferromagnetic, like in $\text{Ca}_2\text{MnO}_4.$ ¹⁷ Fast cooling through T_N has no observable

effects on the 3D order in the other three samples, except for slight hysteresis for $x=0.27$ at the A-OAF phase boundary.

B. Order in 2D

In Fig. 2 the ridge intensity at $Q=(1,0,0.4)$ is shown as a function of the temperature for all four specimens. In Fig. 3, we have plotted ridge intensities near T_N versus the reduced temperature $\epsilon=T/T_N-1$, with T_N deduced from the (100) Bragg intensities, in part with larger counting times ($x=0.18$). The asymmetric peak for $x=0.55$ points to regular 2D Ising critical behavior, whereas for $x=0.27$, closer to $x_c=0.22$, the intensity maximum has broadened, but remains asymmetric. A similar broadening is seen when going from $x=0$ to 0.12. In all these cases, the ridge scattering peaks slightly above $T_N(x)$, as is commonly observed in 2D compounds with small smearing of the phase transition. By contrast, the ridge scattering in the $x=0.18$ specimen can hardly be characterized as being critical, the data showing a broad hump around $\epsilon=0$. The associated slow rise of the 3D order has already been noted in connection with Fig. 1. To bring about the point more clearly, the relevant data of these (100) Bragg reflections have also been inserted in Fig. 3.

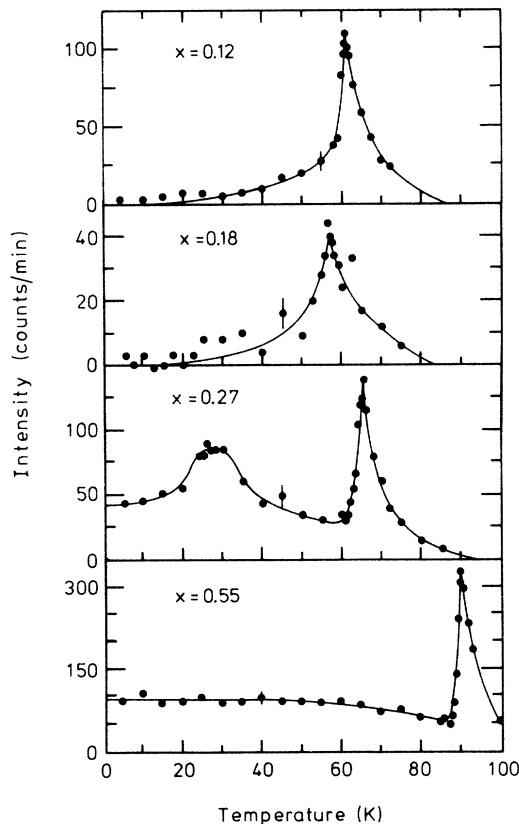


FIG. 2. Temperature dependence of the ridge scattering intensity at $Q=(1,0,0.4)$. Note the different scales of the abscissae.

With regard to the $x=0.27$ sample, apart from the critical scattering around T_N , a very broad maximum in the intensity is observed around T_L (Fig. 2). The observed temperature dependence is independent of the cooling rate, which was below 1 K/min. The second intensity maximum, here observed in a quasielastic double-axis experiment, is not due to ordinary critical scattering, as the width of the ridge essentially equals the instrumental resolution below 60 K. Furthermore, in a triple-axis experiment with zero-energy transfer,⁸ the maximum barely shows up, proving directly that it is, to a large extent, associated with inelastic scattering. Indeed, in a separate inelastic scattering experiment¹⁸ the $q=0$ spin-wave gap of the lowest branch is found to vanish upon approaching T_L from below. At 4.2 K there remains a finite elastic contribution to the ridge, implying that, in part, the spins fail to achieve complete 3D order, but order in separate a, b layers only. A similar residual scattering is observed for $x=0.55$ over a wide range of temperatures, even at the slowest cooling rates employed. Here, a cursory triple-axis experiment shows that the scattering at

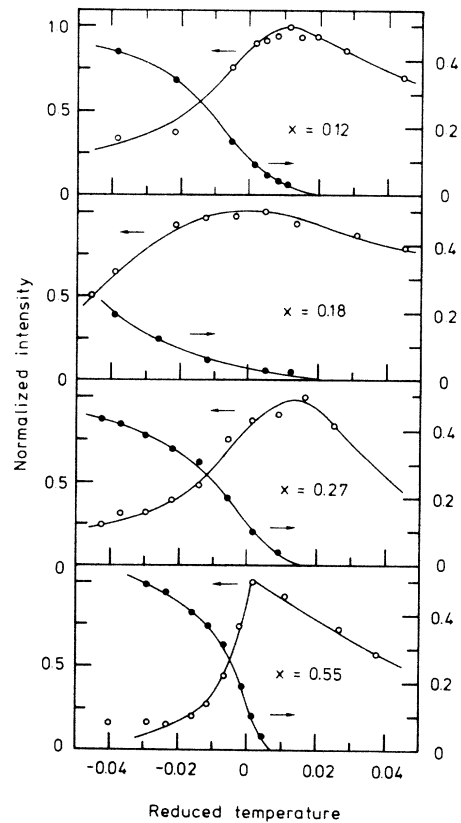


FIG. 3. Ridge scattering intensity at $Q=(1,0,0.4)$ near T_N vs the reduced temperature (open circles, left-hand scale). Background is subtracted. Intensities are normalized to facilitate comparison of the shape of the maxima. Also inserted are the (100) Bragg intensities normalized to zero temperature (solid circles, right-hand scale) to emphasize the slow rise of the order parameter for $x=0.18$.

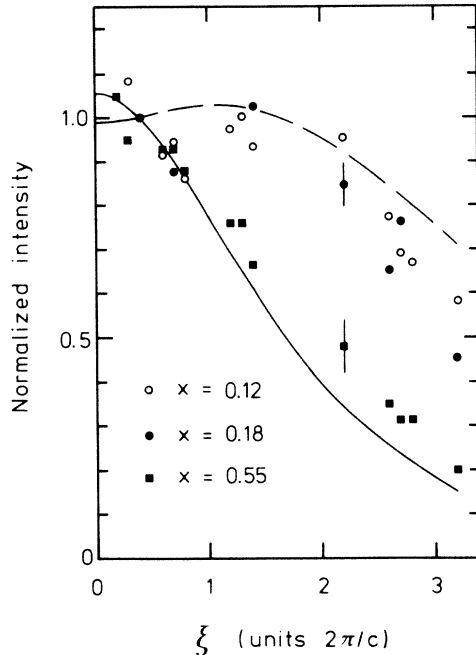


FIG. 4. Scattering intensity along the ridge $Q=(1,0,\xi)$ in the critical regime for $x=0.12$, 0.18 , and 0.55 , taken at 61.0 , 59.0 , and 93.0 K, respectively. Solid and dashed curves represent the calculated intensities for axial and in-layer components, respectively. Data and curves are normalized to $\xi=0.4$.

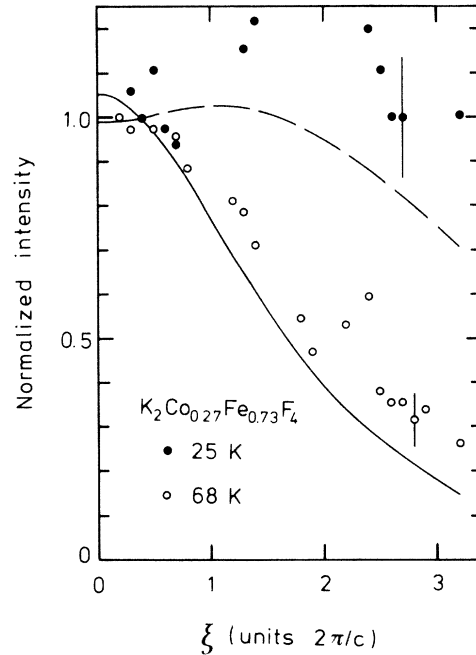


FIG. 5. Same as Fig. 4, but scans along the ridge $Q=(1,0,\xi)$ for $x=0.27$ at 25 and 68 K.

$Q=(1,0,0.4)$ is elastic at 4.2 , 70 , and 85 K. At 4.2 K no residual scattering has been observed in the $x=0.12$ and 0.18 cases.

Extensive scans along the ridge $Q=(1,0,\xi)$, with ξ running from 0 to 3.25 , were made at a few selected temperatures to establish, by a comparison with calculated results, which components of the spin invoke the scattering (Figs. 4 and 5). In the calculations, the ξ dependence of the cross section for quasielastic scattering is computed for 2D arrays of spins correlated in space with the spins directed along either, with equal probability, the a and b axes or along the c axis. In Fig. 4, data at temperatures just above T_N are collected, together with the computed dependences. It is confirmed that the $x=0.55$ sample undergoes a transition to the A phase. (An analysis of the ridge profile in the a^* direction above T_N yielded the critical exponents $\nu=0.7\pm 0.2$ and $\gamma=1.5\pm 0.3$ for the correlation length and the susceptibility, respectively.) Similarly, for $x=0.12$ and 0.18 the scattering is due to the transverse components, consistent with a transition to the PL state. For $x=0.27$ the intensity distribution along the ridge differs markedly around T_L and T_N (Fig. 5). The critical fluctuations at 68 K clearly are of the axial type, in accordance with a transition to the A phase. By contrast, at 25 K mainly the transverse components contribute, consistent with a transition to the OAF phase at T_L . Surprisingly, however, even near T_N the scattering is—to a considerable part—due to long-range-correlated transverse spin components.

IV. CONCLUDING REMARKS

The most interesting part of the phase diagram of $K_2Co_xFe_{1-x}F_4$ is the portion with x close to the multicritical concentration $x_c=0.22$. The specimens with $x=0.18$ and 0.27 studied above are representative examples of this regime. The critical phenomena in the systems with $x=0.12$ and 0.55 do not markedly deviate from those in the pure counterparts K_2FeF_4 and K_2CoF_4 . For $x=0.18$ the susceptibility does not show the characteristic divergence, although at low temperatures ultimately long-range 3D order develops. Clearly, for x just below x_c , the nearly balanced anisotropies marginally leave the spins in the layers, and thus the system resembles the 2D XY model. The ordering may be further disturbed by the local randomness. It should be emphasized that for these phenomena to occur the low dimensionality is crucial. In corresponding 3D systems, the ordering processes have not been found to change notably upon cancellation of the anisotropies.³ A crossover from 2D Ising to 2D XY behavior has, however, been identified in the diluted system $K_2Fe_xZn_{1-x}F_4$,¹⁹ where the critical scattering is similarly suppressed, and dynamic behavior persists in a substantial range of temperatures below T_N . Concerning $K_2Co_{0.18}Fe_{0.82}F_4$, we finally note that, despite the closeness of x_c , no transition from the PL phase into the OAF phase has been observed. This is in accord with a mean-field calculation of the PL-OAF phase boundary with adjustment of the Co-Fe exchange to match the measured phase diagram, which indicates this line to be exceptionally steep (slope of 60 K per percent in x).¹³

At the other side of the multicritical point, crossover

only occurs very close to x_c . In $K_2Co_{0.27}Fe_{0.73}F_4$, no drastic modification of the critical behavior upon entering the A phase at T_N is observed. In assessing the nature of the subsequent transition to the OAF phase at T_L , the evidence must be differentiated according to the length and time scales with which the experimental technique probes the spins. With Mössbauer spectroscopy,¹² the transverse components are seen as dynamic on a time scale 10^{-8} s between T_L and T_N . From the present neutron-diffraction experiments, by contrast, these components are found already correlated over at least 100 in-layer lattice spacings within 10^{-11} s. That is, the spin fluctuations are substantially slowed down as compared to the fluctuations preceding the transition at T_N . In the absence of a coupling between the already ordered axial components and the transverse ones,^{3,20} the orthogonal

magnetizations would, of course, order independently, each associated with a second-order transition.⁵ On the other hand, a strong coupling invokes a single transition involving both components.³ For weak coupling, therefore, the A-OAF transition remains of second order, but one preceded by hindered fluctuations. In view of the high crystalline symmetry, this presumably is the case in $K_2Co_{0.27}Fe_{0.73}F_4$.

ACKNOWLEDGMENTS

Technical assistance by H. H. A. Plas and crystal growing by C. R. de Kok are gratefully acknowledged. We have benefited from a discussion with Professor R. A. Cowley. We further acknowledge discussions with Dr. B. J. Dikken.

¹F. Matsubara and S. Inawashiro, *J. Phys. Soc. Jpn.* **42**, 1529 (1977); T. Oguchi and T. Ishikawa, *ibid.* **45**, 1213 (1978); Y. Someya, *ibid.* **50**, 3897 (1981).

²A. Aharony and S. Fishman, *Phys. Rev. Lett.* **37**, 1587 (1976); S. Fishman and A. Aharony, *Phys. Rev. B* **18**, 3507 (1978).

³P. Wong, P. M. Horn, R. J. Birgeneau, and G. Shirane, *Phys. Rev. B* **27**, 428 (1983).

⁴A. Ito, Y. Someya, and K. Katsumata, *Solid State Commun.* **36**, 681 (1980); A. Ito, S. Morimoto, Y. Someya, H. Ikeda, Y. Syono, and H. Takei, *ibid.* **41**, 507 (1982); Y. Someya, A. Ito, and K. Katsumata, *J. Phys. Soc. Jpn.* **52**, 254 (1983).

⁵K. Katsumata, H. Yoshizawa, G. Shirane, R. J. Birgeneau, *Phys. Rev. B* **31**, 316 (1985).

⁶L. Bevaart, E. Frikkee, J. V. Lebesque, and L. J. de Jongh, *Phys. Rev. B* **18**, 3376 (1978).

⁷W. A. H. M. Vlak, E. Frikkee, A. F. M. Arts, and H. W. de Wijn, *J. Phys. C* **16**, L1015 (1983).

⁸S. A. Higgins, R. A. Cowley, M. Hagen, J. Kjems, U. Dürr, and K. Fendler, *J. Phys. C* **17**, 3235 (1984).

⁹K. Fendler, W. P. Lehmann, R. Weber, and U. Dürr, *J. Phys.*

C **15**, L533 (1982); **17**, 4019 (1984).

¹⁰H. Ikeda and K. Hirakawa, *Solid State Commun.* **14**, 529 (1974).

¹¹M. P. H. Thurlings, E. Frikkee, and H. W. de Wijn, *Phys. Rev. B* **25**, 4750 (1982).

¹²W. A. H. M. Vlak, B. J. Dikken, A. F. M. Arts, and H. W. de Wijn, *Phys. Rev. B* **31**, 4496 (1985).

¹³K. Fendler and G. von Eynatten, *Z. Phys. B* **54**, 313 (1984).

¹⁴R. J. Birgeneau, J. Als-Nielsen, and G. Shirane, *Phys. Rev. B* **16**, 280 (1977).

¹⁵W. A. H. M. Vlak, M. J. van Dort, A. F. M. Arts, and H. W. de Wijn (unpublished).

¹⁶E. J. Samuelsen, *J. Phys. Chem. Solids* **35**, 785 (1974).

¹⁷D. E. Cox, G. Shirane, R. J. Birgeneau, and J. B. MacChesney, *Phys. Rev.* **188**, 930 (1969).

¹⁸S. A. Higgins, W. A. H. M. Vlak, M. Hagen, R. A. Cowley, A. F. M. Arts, and H. W. de Wijn (unpublished).

¹⁹B. J. Dikken, A. F. M. Arts, H. W. de Wijn, W. A. H. M. Vlak, and E. Frikkee, *Phys. Rev. B* **32**, 5600 (1985).

²⁰D. Mukamel, *Phys. Rev. Lett.* **46**, 845 (1981).